Investigation of a transition from steady convection to chaos in porous media using piecewise variational iteration method

Mohamed M. Mousa, Aidarkhan Kaltayev and Shahwar F. Ragab

Abstract—In this paper, a new dependable algorithm based on an adaptation of the standard variational iteration method (VIM) is used for analyzing the transition from steady convection to chaos for low-to-intermediate Rayleigh numbers convection in porous media. The solution trajectories show the transition from steady convection to chaos that occurs at a slightly subcritical value of Rayleigh number, the critical value being associated with the loss of linear stability of the steady convection solution. The VIM is treated as an algorithm in a sequence of intervals for finding accurate approximate solutions to the considered model and other dynamical systems. We shall call this technique as the piecewise VIM. Numerical comparisons between the piecewise VIM and the classical fourth-order Runge–Kutta (RK4) numerical solutions reveal that the proposed technique is a promising tool for the nonlinear chaotic and nonchaotic systems.

Keywords—Variational iteration method; Free convection; Chaos; Lorenz equations.

I. INTRODUCTION

POROUS-media convection is of interest for a variety of geological and engineering applications, and this particular model has proven to be a useful quantitative model over a range of Rayleigh numbers (*Ra*) [1]. Its dynamics and bifurcation structure have been thoroughly explored theoretically and computationally for low-to-intermediate Rayleigh numbers both for the standard Rayleigh–Bénard problem studied here [2], and more recently for an open-top version of the problem [3]. Moreover, buoyancy-driven flows such as thermal convection are of great importance for a wide range of phenomena in geophysical, astrophysical and engineering applications. Rayleigh–Bénard convection in particular is a fundamental paradigm for nonlinear dynamics including instabilities and bifurcations, pattern formation, chaotic dynamics and developed turbulence [4]. Despite the great deal of attention that has been devoted to it, the dynamics of high-Rayleigh-number convective turbulence and the associated enhancement of the heat transport still present challenges for theory and experiment [5].

M. M. Mousa is with the Department of Basic Science, Benha High Institute of Technology, Benha University, 13512, Egypt (corresponding author to provide e-mail: dr.eng.mmmm@gmail.com).

A. Kaltayev is with Department of Mechanics, al-Farabi Kazakh National University, 39/47 Masanchi 050012, Almaty, Kazakhstan (e-mail: Aidarkhan. Kaltayev@kaznu.kz).

S. F. Ragab is with the Department of Engineering Mathematics and Physics, Faculty of Engineering, Cairo University, Giza, Egypt (e-mail: shah_ragb@yahoo.com).

The objective of the present paper is to report the results of low-to-intermediate Rayleigh numbers transition to chaos in a fluid saturated porous layer and heated from below. This is accomplished by adopting proposed piecewise variational iteration, to solve the set of ordinary differential equations obtained via a truncated Galerkin expansion. The truncated Galerkin expansion is shown to be equivalent to Lorenz equations applicable for convection in pure fluids (nonporous domains) [6]. Vadasz and Olek investigated the weak turbulence and chaos for low prandtl number gravity driven convection in porous media using Adomian's decomposition method (ADM) [7]. For the problem considered in the present paper, the results show that the transition from steady convection to chaos is sudden.

The variational iteration method (VIM) was first proposed by He [8, 9], and was successfully applied to autonomous ordinary differential equations [10], to nonlinear polycrystalline solids [11], to various kinds of nonlinear problems and other fields [12–21]. The VIM has many merits and advantages over the (ADM) [24]. The method has been shown to solve effectively, easily, and accurately a large class of nonlinear problems, generally one or two iterations lead to high accurate solutions. This method is, in fact, a modifying of the general Lagrange multiplier method into an iteration method, which is called correction functional. For a relatively comprehensive survey on the method, new interpretation, and new development, the reader is referred to the review articles [22, 23].

The rest of this paper is organized as follows: In § 2 we set out the details of the model, present some basic definitions and represent model solution in terms of a truncated Galerkin expansion. In § 3 we discuss the stability of reduced set of ODEs that describe the dynamics of time evolution of the amplitude's solution. In § 4 we describe the basic idea of the classical VIM, suggest an algorithm of the proposed piecewise VIM and apply the proposed algorithm for solving reduced set of ODEs to demonstrate its dynamics. In § 5 we present the obtained results and demonstrate the accuracy of the piecewise VIM against the Maple's built-in fourth-order Runge–Kutta (RK4) procedure for the solutions of model equations. The effect of Rayleigh number on the model dynamics and on the transition from steady convection to chaos is also illustrated in section 5. The concluding § 6 is a brief summary of the obtained results.

II. STATEMENT OF THE PROBLEM

A fluid saturated porous layer subject to gravity and heated from below as presented in Fig. 1 is considered. For convenience, we consider a layer of fluid-saturated porous material confined between two horizontal plates at $z = 0$, $z = 1$. The temperature field $T(\mathbf{x}, t)$ the velocity field $\mathbf{v}(\mathbf{x}, t) = u\,\mathbf{i} + v\,\mathbf{j} + w\,\mathbf{k}$, and the pressure $P(\mathbf{x}, t)$ evolve according to

$$\nabla . \mathbf{v} = 0, \tag{1}$$

$$\gamma a \frac{\partial \mathbf{v}}{\partial t} = -\nabla P - \mathbf{v} + \mathrm{R}a\,T\,\mathbf{k}, \tag{2}$$

$$\frac{\partial T}{\partial t} + \mathbf{v} . \nabla T = \nabla^2 T \tag{3}$$

where $\mathbf{k}$ is the unit vector in the z direction, $\mathrm{R}a$ is the porous media gravity related Rayleigh number, and γa is a nondimensional acceleration coefficient,

$$\gamma a = \frac{c_a \mathrm{D}a}{\sigma \,\mathrm{Pr}_m}, \tag{4}$$

where c_a is the acceleration coefficient, $\mathrm{D}a$ is the Darcy number, σ is the heat capacity ratio and Pr_m is the porous media Prandtl number. It's obvious that the nondimensional acceleration coefficient γa is equivalent to the inverse of Darcy–Prandtl number.
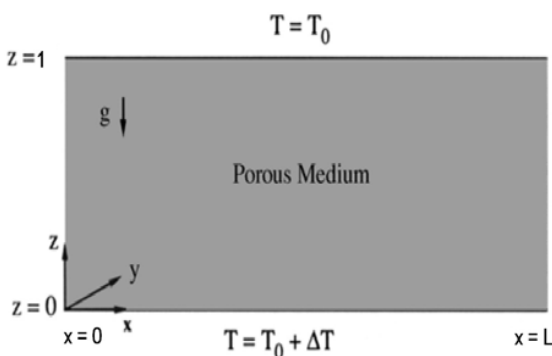

Fig. 1. Fluid-saturated porous medium heated from below

This model is obtained from the Darcy–Oberbeck–Boussinesq equations after making nondimensionalizing and taking other standard assumptions (local thermal equilibrium, negligible heating from viscous dissipation, negligible radiative effects, etc.) [1]. Assuming that all the boundaries are rigid, so the solution must follow the impermeability conditions there, that is $\mathbf{v} . \mathbf{n} = 0$ on the boundaries, where $\mathbf{n}$ is a unit vector normal to the boundary. For convenience, let the temperature boundary conditions are: $T = 1$ at $z = 0$, $T = 0$ at $z = 1$ and $\nabla T . \mathbf{n} = 0$ on all other walls representing the insulation condition on these walls.

As a matter of convenience, we compute two-dimensional solutions of the model equations (1), (2), (3), dropping the y-dependence of all variables and setting $v = 0$.

Moreover, for convenience, we recast the problem using the deviation of the temperature field from the conduction solution, $\Theta = T - (1 - z)$, and the stream function ψ where $(u, w) = (\psi_z, -\psi_x)$. Hence, the boundary conditions for these new variables are $\Theta|_{z=0,1} = 0$ and $\psi = 0$ on all solid boundaries. Using the new variables and applying the curl $(\nabla \times)$ operator on Eq. (2) yields the following system of PDEs from Eqs. (1)–(3):

$$\gamma a \frac{\partial}{\partial t}\left(\frac{\partial^2 \psi}{\partial x^2} + \frac{\partial^2 \psi}{\partial z^2}\right) + \frac{\partial^2 \psi}{\partial x^2} + \frac{\partial^2 \psi}{\partial z^2} + Ra \frac{\partial \Theta}{\partial x} = 0, \tag{5}$$

$$\frac{\partial \Theta}{\partial t} + \frac{\partial \psi}{\partial z}\frac{\partial \Theta}{\partial x} - \frac{\partial \psi}{\partial x}\frac{\partial \Theta}{\partial z} + \frac{\partial \psi}{\partial x} = \frac{\partial^2 \Theta}{\partial x^2} + \frac{\partial^2 \Theta}{\partial z^2}. \tag{6}$$

The set of PDEs (5) and (6) form a nonlinear coupled system which together with the corresponding boundary conditions accepts a basic motionless conduction solution.

Our goal is to investigate the transition from steady convection to chaos that appears from the solution of this nonlinear coupled system of PDEs. To obtain the solution to the system of PDEs (5) and (6), we represent ψ and Θ in the form

$$\psi(x, z, t) = X(t)\sin\left(\frac{\pi x}{L}\right)\sin(\pi z), \tag{7}$$

$$\Theta(x, z, t) = Y(t)\cos\left(\frac{\pi x}{L}\right)\sin(\pi z) + Z(t)\sin(2\pi z), \tag{8}$$

where L is the length of the porous layer along x direction.

This representation is equivalent to a Galerkin expansion of the solution in both x and z irections, truncated when $i+j=2$, where i is the Galerkin summation index in the x direction and j is the Galerkin summation index in the z direction. This expansion is equivalent to that considered by Lorenz [6] to investigate thermal convection in a layer heated from below (the Bénard problem). It is obvious that the solution presented in (7) and (8) satisfy boundary conditions. Substituting solutions (7) and (8) into Eqs. (5) and (6), separately multiplying the equations by the orthogonal eigenfunctions

$$\sin\left(\frac{\pi x}{L}\right)\sin(\pi z),\ \cos\left(\frac{\pi x}{L}\right)\sin(\pi z),\ \sin(2\pi z)$$

and integrating them over the domain, that is, $\int_{z=0}^{z=1}\int_{x=0}^{x=L}(.)\,\mathrm{d}x\,\mathrm{d}z$, yields a set of three ODEs for the time evolution of the amplitudes $X(t)$, $Y(t)$ and $Z(t)$ in the following form

$$\frac{d}{dt}X(t) + \frac{RY(t) + X(t)}{\gamma a} = 0, \tag{9}$$

$$\frac{d}{dt}Y(t) + \frac{\pi^2(1 + L^2)Y(t)}{L^2} + \frac{\pi X(t)}{L} + \frac{\pi^2 X(t)Z(t)}{L} = 0, \tag{10}$$

$$\frac{d}{dt}Z(t)+4\pi^2 Z(t)-\frac{1}{2}\frac{\pi^2 X(t)Y(t)}{L}=0, \tag{11}$$

where $R=\mathrm{R}a\,L/\pi\left(1+L^2\right)$ is the scaled Rayleigh number.

Before studying the behavior of ODEs (9)–(11) corresponding to arbitrary initial conditions using the proposed piecewise VIM and comparing the results with that obtained by RK4, we will discus the solutions stability of the ODEs system.

III. STABILITY ANALYSIS

We proceed to find the fixed points (steady solutions) that occur when $\dfrac{dX}{dt}=\dfrac{dY}{dt}=\dfrac{dZ}{dt}=0$, and evaluate their stability. The fixed points of the system are $X_1^*=Y_1^*=Z_1^*=0$ corresponding to the motionless conduction solution, and $X_{2,3}^*=\mp2\sqrt{2\left(\dfrac{RL}{\pi}-\left(1+L^2\right)\right)}$,

$$Y_{2,3}^*=\pm\frac{2}{R}\sqrt{2\left(\frac{RL}{\pi}-\left(1+L^2\right)\right)}, \qquad Z_{2,3}^*=\frac{1+L^2}{RL}-\frac{1}{\pi}$$

corresponding to the steady convective solutions.

The stability of the fixed point associated with the motionless solution $\left(X_1^*,Y_1^*,Z_1^*\right)$ is controlled by the zeros of the following characteristic polynomial for the eigenvalues, $\lambda_i,\ \left(i=1,2,3\right)$:

$$\left(\lambda+4\pi^2\right)[\gamma a\,L^2\lambda^2+\left(\pi^2\gamma a\left(1+L^2\right)+L^2\right)\lambda \\ +\pi^2\left(1+L^2\right)-\pi RL]=0. \tag{12}$$

The roots of Eq. (12) provides the stability condition for the motionless solution. As usual,

$$\mathrm{Re}\left\{\lambda_1,\lambda_2\ \text{and}\ \lambda_3\right\}\ <\ 0\ \Rightarrow\ \text{stable}$$

$$\mathrm{Re}\left\{\lambda_1,\lambda_2\ \text{or}\ \lambda_3\right\}\ >\ 0\ \Rightarrow\ \text{unstable}$$

Therefore it easy to verify that $X_1^*=Y_1^*=Z_1^*=0$ is stable for $0<R<\pi\left(1+L^2\right)/L$ and unstable for $R>\pi\left(1+L^2\right)/L$. Thus the critical value of R, where the motionless solution loses stability and the convection solution takes over, is obtained as $R_{c1}=R_{cr}=\pi\left(1+L^2\right)/L$, which corresponds to

$$\mathrm{R}a_{cr}=\left[\pi\left(1+L^2\right)/L\right]^2. \tag{13}$$

Form Eq. (13), it is obvious that the well known critical Rayleigh number $\mathrm{R}a_{cr}=4\pi^2$ that mentioned by many authors (see [1,5,7]) can be obtained by setting L to unity, i.e. $R_{c1}=2\pi$.

We now calculate the stability of the fixed points of the convection solution $\left(X_{2,3}^*,Y_{2,3}^*,Z_{2,3}^*\right)$. The stability of this solution is controlled by the following cubic equation

$$\lambda^3+\frac{\left(L^2\left(1+5\pi^2\gamma a\right)+\pi^2\gamma a\right)}{\gamma a L^2}\lambda^2+\frac{4\pi^2\left(\pi\gamma aR+L\right)}{L\gamma a}\lambda \\ +\frac{8\pi^3\left(RL-\pi\left(1+L^2\right)\right)}{\gamma a L^2}=0. \tag{14}$$

The former equation yields one real root and two complex conjugate roots. The real root is negative over the whole range of parameters' values only when $R>\pi\left(1+L^2\right)/L$. For the two complex roots, we found that their real part is negative for $R>\pi\left(1+L^2\right)/L$ and becomes non-negative at a value of

$$R>R_{c2}=\frac{L\left(L^2\left(1+7\pi^2\gamma a\right)+3\pi^2\gamma a\right)}{\pi\gamma a\left(L^2\left(1-5\pi^2\gamma a\right)-\pi^2\gamma a\right)}, \tag{15}$$

which is the condition of instability for the convective case. This condition, which exists only for $\gamma a<L^2/\pi^2\left(5L^2+1\right)$, gives the critical value of R for which steady convection becomes unstable. So, the convective state is stable for $\pi\left(1+L^2\right)/L<R<R_{c2}$ and unstable for $R>R_{c2}$.

As an example, for $L=1$ and $\gamma a=0.005$, the fixed points corresponding to the motionless solution loss their stability at $R_{c1}=2\pi$, however the loss of stability of the convection fixed points is evaluated from Eq. (15) to be $R_{c2}\simeq135$.

IV. PIECEWISE VARIATIONAL ITERATION METHOD

A. Brief description of the variational iteration method

In order to illustrate the basic concepts of VIM, the following nonlinear partial differential equation can be considered

$$Lu(x,t)+Ru(x,t)+Nu(x,t)=g(x,t), \tag{16}$$

where L is a linear time derivative operator, R is a linear operator which has derivatives with respect to x and t, N is a nonlinear differential operator, and $g(x,t)$ is a source inhomogeneous term. According to the VIM [8–23], we can construct the following iteration formula for Eq. (16):

$$u_{n+1}(x,t)=u_n(x,t)+\int_0^t\lambda\left\{Lu_n(x,\tau)+R\widetilde{u}_n(x,\tau)+N\widetilde{u}_n(x,\tau)-g(x,\tau)\right\}d\tau, \tag{17}$$

where the parameter λ is a general Lagrange's multiplier, which can be identified optimally via the variational theory, the subscript n denotes the nth-order approximation, and $\widetilde{u}_n$

is considered as a restricted variation [8–23] which means $\widetilde{\delta u_n} = 0$.

It is obvious now that the main steps of He's VIM require first the determination of the Lagrange's multiplier λ that will be identified optimally. Having determined λ, the successive approximations u_{n+1}, $n \geq 0$, of the solution u will be obtained upon using any selective function u_0.

The main drawback of standard VIM is that, like any other methods based on series solution, the series can be rapidly convergent in a very small region, it has very slow convergence rate in the wider region and the truncated series solution is an inaccurate solution in that region, which will greatly restrict the application area of the method.

B. Proposed piecewise variational iteration method

The proposed piecewise VIM is suitable only for solving initial value problems corresponding to systems of ODEs. The convergence of the VIM series approximation u_{n+1}, $n \geq 0$ obtained from the iteration formula (17) is difficult to assess a priori. Irrespective of this difficulty, the practical need to compute numerical values for the solution at different values of time requires the truncation of the series and therefore its convergence needs to be established in each particular case. To achieve this goal, the VIM can be used as an algorithm for the approximation of ODEs response in a sequence of time intervals $[t_0, t_1), [t_1, t_2), ..., [t_{m-1}, t_m)$ such that the solution at t_p is taken as initial condition in the interval $[t_p, t_{p+1})$ which follows. To carry out the iterations for each subinterval of equal length $\Delta t = t_m - t_{m-1}$, where $m = 1, 2, ...$ and t_m is a value of maximum time (right-end point), we had to choose the initial approximation of Eq. (17) as a constant c that can be identified later,

$$u_0(t) = c. \quad (18)$$

Once obtaining the Lagrange's multiplier λ and substituting initial approximation (18) into the correction formula (17), one can obtain the desired successive approximation $u_{n+1}(t; c)$. Our goal now is to make the approximate solution $u_{n+1}(t; c)$ accurate for each subinterval $[t_{m-1}, t_m)$, $m = 1, 2, ...$. To achieve this goal, we proposed setting t in $u_{n+1}(t; c)$ as $t - t^*$, where t^* is the left-end point of each subinterval. Hence, we obtain a solution $u_{n+1}(t - t^*; c)$ for each subinterval $[t^*, t^* + \Delta t)$. The second step of the algorithm is how to obtain the value of c for each subinterval. This can be easily done by equating c in $u_{n+1}(t - t_0; c)$ with the given initial condition $u(t_0) = c_0$; equating c in $u_{n+1}(t - t_1; c)$ with $u_{n+1}(t_1 - t_0; c_0) = c_1$;

equating c in $u_{n+1}(t - t_2; c)$ with $u_{n+1}(t_2 - t_1; c_1) = c_2$ and so on until calculating c in $u_{n+1}(t - t_{m-1}; c)$ as $u_{n+1}(t_{m-1} - t_{m-2}; c_{m-2}) = c_{m-1}$. Therefore, we have m solutions $u_{n+1}(t - t_0; c_0)$, $u_{n+1}(t - t_1; c_1), ..., u_{n+1}(t - t_{m-1}; c_{m-1})$ for m subintervals $[t_0, t_1), [t_1, t_2), ..., [t_{m-1}, t_m)$ respectively. This algorithm can be easily implemented in any symbolic software such as Maple and Mathematica.

C. Application of the piecewise variational iteration method

According to the classical VIM, the variational iteration formulas of the ODEs (9)–(11) can be constructed as follows,

$$X_{i+1}(t) = X_i(t) + \int_0^t \lambda_1 \left(\frac{d}{d\tau} X_i(\tau) + \frac{R\tilde{Y}_i(\tau) + \tilde{X}_i(\tau)}{\gamma a} \right) d\tau, \quad (19)$$

$$Y_{i+1}(t) = Y_i(t) + \int_0^t \lambda_2 \left(\frac{d}{d\tau} Y_i(\tau) + \frac{\pi^2(1+L^2)\tilde{Y}_i(\tau)}{L^2} \right.$$
$$\left. + \frac{\pi\tilde{X}_i(\tau)}{L} + \frac{\pi^2\tilde{X}_i(\tau)\tilde{Z}_i(\tau)}{L} \right) d\tau, \quad (20)$$

$$Z_{i+1}(t) = Z_i(t) + \int_0^t \lambda_3 \left(\frac{d}{d\tau} Z_i(\tau) + 4\pi^2\tilde{Z}_i(\tau) \right.$$
$$\left. - \frac{1}{2}\frac{\pi^2\tilde{X}_i(\tau)\tilde{Y}_i(\tau)}{L} \right) d\tau, \quad (21)$$

where λ_1, λ_2 and λ_3 are general Lagrange's multipliers, which can be identified optimally via the variational theory. Making the correction formulas (19)–(21) stationary by multiplying them by δ, yields the following stationary conditions

$$\frac{d\lambda_i(\tau)}{d\tau} = 0, \quad 1 + \lambda_i(\tau)|_{\tau=t} = 0, \quad i = 1, 2, 3 \quad (22)$$

Therefore, the Lagrange's multipliers can be identified as $\lambda_1 = \lambda_2 = \lambda_3 = -1$.

Based on the proposed algorithm of the piecewise VIM, we assumed the initial approximations of the iteration formulas as constants,

$$X_0(t) = c_1, \ Y_0(t) = c_2, \ Z_0(t) = c_3. \quad (23)$$

Substituting initial approximations (23) into iteration formulas (19)–(21), obtaining only two iterations approximate solution and setting t as $t - t^*$ yields

$$X_2(t - t^*; \mathbf{c}) = \frac{1}{2}\left[\frac{R\pi^2 c_2}{\gamma a} + \frac{R\pi^2 c_2}{L^2\gamma a} + \frac{c_1}{\gamma a^2} + \frac{R\pi c_1}{L\gamma a} + \frac{R\pi^2 c_1 c_3}{L\gamma a} \right.$$
$$\left. + \frac{Rc_2}{\gamma a^2} \right](t - t^*)^2 - \frac{1}{\gamma a}[c_1 + Rc_2](t - t^*) + c_1, \quad (24)$$

$$Y_2(t-t^*;\mathbf{c})=\frac{\pi^4}{6L\gamma a}[\frac{c_1^2c_2}{L}-8c_3Rc_2+\frac{Rc_2^2c_1}{L}-8c_1c_3](t-t^*)^3$$

$$+\frac{1}{2}[\frac{\pi^4c_2}{L^4}+\frac{2\pi^4c_2}{L^2}+\frac{\pi^3c_1}{2L^3}+\pi^4c_2+\frac{\pi^3c_1}{L}+\frac{5\pi^4c_1c_3}{L}$$

$$+\frac{\pi Rc_2}{L\gamma a}+\frac{\pi c_1}{L\gamma a}+\frac{\pi^4c_1^2c_2}{2L^2}+\frac{\pi^2c_3Rc_2}{L\gamma a}+\frac{\pi^2c_1c_3}{L\gamma a}+\frac{\pi^4c_1c_3}{L^3}](t-t^*)^2$$

$$-[\frac{\pi c_1}{L}+\frac{\pi^2c_1c_3}{L}+\frac{\pi^2c_2}{L^2}+\pi^2c_2](t-t^*)+c_2,$$

$$Z_2(t-t^*;\mathbf{c})=\frac{\pi^3}{6L\gamma a}[\pi c_1c_2+\pi Rc_2^2+\frac{Rc_2c_1}{L}+\frac{\pi Rc_2c_3}{L}+\frac{c_1^2}{L}+\frac{\pi c_1^2c_3}{L}+$$

$$\frac{\pi c_1c_2}{L^2}+\frac{\pi Rc_2^2}{L^2}](t-t^*)^3-\frac{1}{4}[\frac{\pi^4c_1^2c_3}{L^2}+\frac{\pi^3c_1^2}{L^2}+\frac{\pi^2c_1c_2}{\gamma a L}-32\pi^4c_3$$

$$+\frac{5\pi^4c_1c_2}{L}+\frac{\pi^2c_2^2R}{\gamma a L}+\frac{\pi^4c_1c_2}{L^2}](t-t^*)^2+[\frac{\pi^2c_1c_2}{2L}-4\pi^2c_3](t-t^*)+c_3,$$

(25)

(26)

where $\mathbf{c}=(c_1,c_2,c_3)$.

According to the second step of the piecewise VIM algorithm, it is easy to calculate the components of the constant vector $\mathbf{c}$ for every subinterval $[t_{m-1},t_m)$, $m=1,2,\dots$ if we set $\mathbf{c}_0=(X(t_0),Y(t_0),Z(t_0))$ which is the vector of the known initial conditions.

V. RESULTS AND DISCUSSION

We shall demonstrate the accuracy of the piecewise VIM against the Maple's built-in RK4 procedure for the solution of model equations (9)–(11). The piecewise VIM algorithm is coded in the computer algebra package Maple. We also fixed the values of the parameters $L=1$, $\gamma a=0.005$ that lead to $R_{c1}=2\pi$, $R_{c2}\simeq135$. The complete solutions for various values of R varying between $1<R\le500$ are computed and illustrating graphically. The time range studied in this work is $[t_0=0, t_m=5]$. All solutions were obtained by using the same initial conditions which were selected to be in the neighborhood of the motionless solution fixed points. As such, the common initial conditions are at $t=0$: $X(0)=Y(0)=Z(0)=0.1$. In this analysis, we attempt to demonstrate the accuracy of piecewise VIM for the solutions of both nonchaotic cases in which $1<R<R_{c2}\simeq135$ and chaotic cases in which $R>R_{c2}$. Based on our preliminary calculations, we select the time step size $\Delta t=0.001$ for $R<135$ and time step size $\Delta t=0.0001$ for $R>135$ in both of piecewise VIM and RK4 method. State space projections of trajectories onto the Y-X, Z-X, and Z-Y planes

for various values of R were carried out using piecewise VIM results up to the maximum time $t_m=5$.

From ODE (10), it is obvious that the amplitude $Y(t)$ depends on the two other amplitudes $X(t)$ and $Z(t)$. Thus, we can demonstrate the accuracy of the piecewise VIM results against RK4 results for the convective case, i.e. $R>R_{c1}=2\pi\simeq6.28$, through comparing only the solution $Y(t)$ obtained by the two methods.

From the graphical comparison between piecewise VIM results and RK4 results of the dependent variable $Y(t)$ shown in Figs. 2–8, It can be observed that the proposed method achieve comparable accuracy compared with the RK4 solutions. For $0<R<R_{c1}\simeq6.28$, it is predicted that the steady state (post-transient) trajectories of $X(t)$, $Y(t)$ and $Z(t)$ will be settle into the values of motionless conduction fixed points $X_1^*=Y_1^*=Z_1^*=0$ as shown in Fig.2. The sequence of events leading to the loss of stability of the steady convection regime is presented in Figs. 3–6 in terms of projections of trajectories (including the transient solution) onto the Y-X, Z-X and Z-Y planes. From Figs. 3–6 we can observe that for various Rayleigh numbers above the loss of stability of the motionless solution ($R>6.28$) the trajectory moves to one of the steady convection points $X=X_{2,3}^*$, $Y=Y_{2,3}^*$ and $Z=Z_2^*$ on a spiral. The spiralling approach towards the fixed point persists increasing the rate of motion in the angular direction with increasing the value of R. It is evident that the trajectory moves towards the fixed point by observing the behavior of $Y(t)$ in the time domain. In Fig. 6, we observe a white hole around the convection fixed point indicating that the maximum time allocated for the computation was not sufficient for the trajectory to reach the fixed point. This result is the first evidence of approaching the transition point. As soon as the value of R approaches the critical value $R_{c2}=135$ we observe that a chaotic regime takes over and the transition from steady convection to chaos occurs as shown in Fig. 7. We notice that this transition occurs at a subcritical value of R (*not shown here*). The chaotic regime persists at $R>135$ and has forms as presented in Figs. 7 and 8.

From Figs. 7(d), 8(c) and 8(d), we conclude that for the chaotic regime and after an initial transient, the behavior of $Y(t)$ settles into an irregular oscillation that persists as $t\to\infty$, but never repeats exactly. This motion is aperiodic and can be considered as a weak turbulence. For detailed understanding of the graphs represent the projection of the solution onto the Y-X plane, Z-X plane and Z-Y plane in case of chaotic regime that appears in Figs. 7(a–c), 8(a) and 8(b), we recommend reading the section concerning with Lorenz equations in [25].
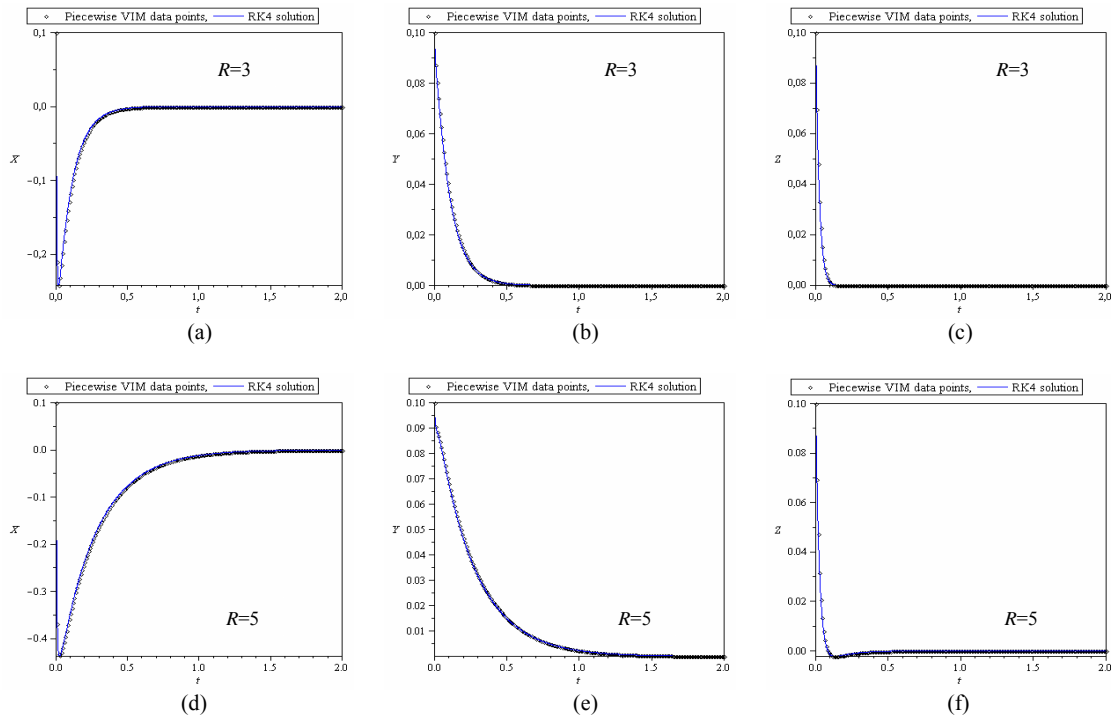
Fig. 2. The evolution of trajectories over time in the state space for R=3 and R=5. The graphs represent a comparison of time-history plots of $X(t)$, $Y(t)$ and $Z(t)$ by present method and RK4 for R=3 in (a)–(c) and for R=5 in (d)–(f)
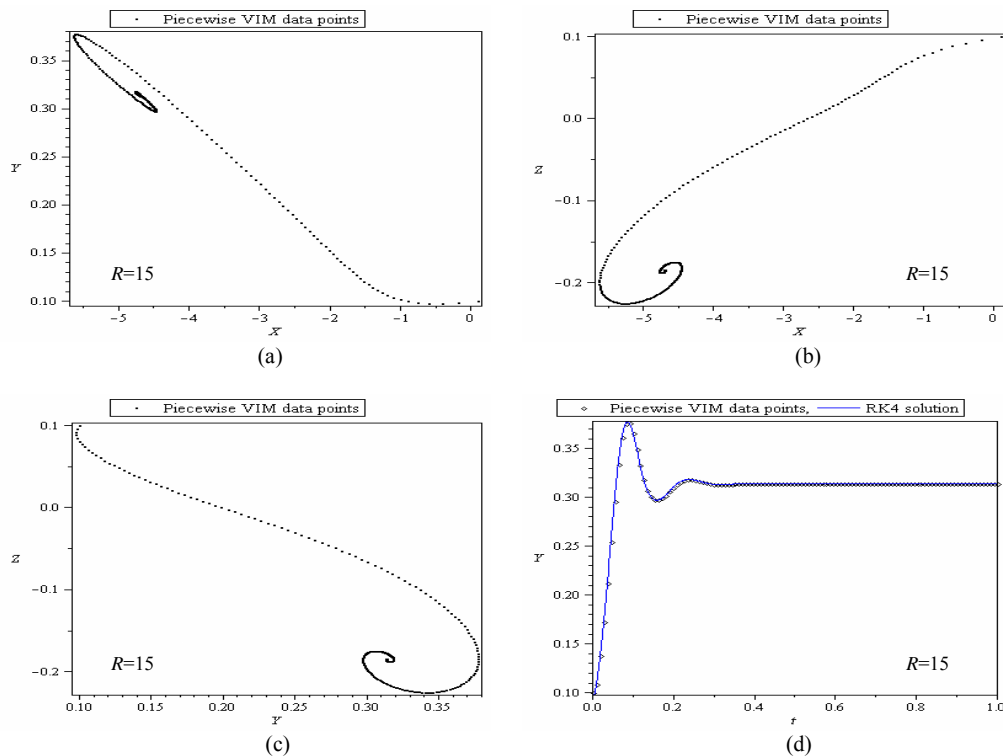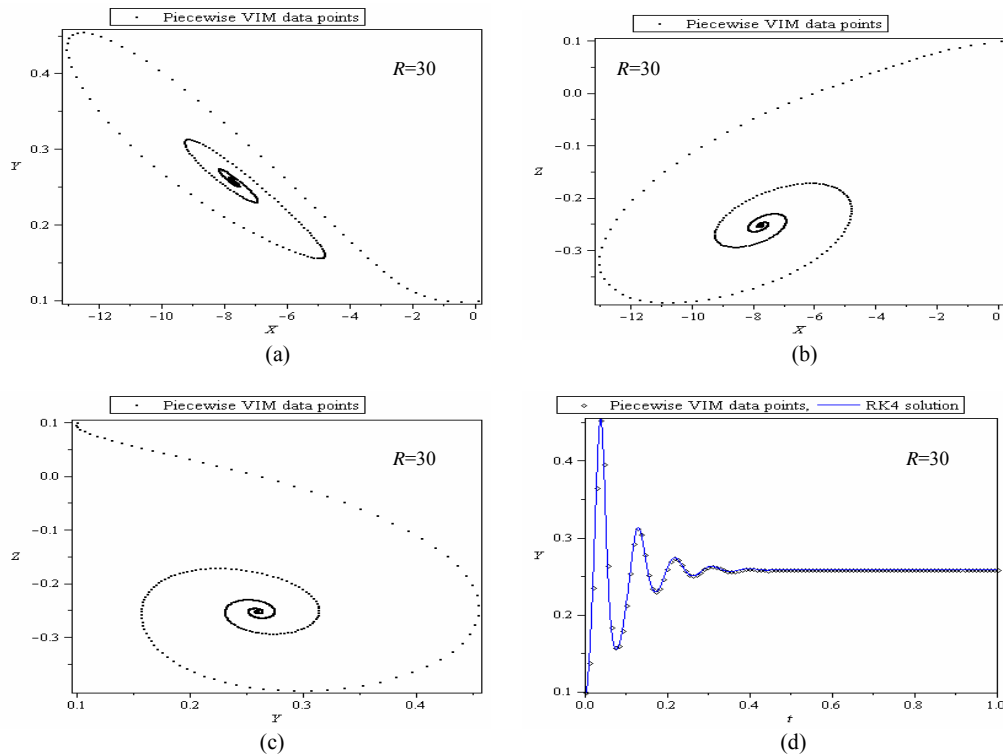

Fig. 3. The evolution of trajectories over time in the state space for R=15 of steady fixed point≈ (−4.71, 0.31, −0.18).
The graphs (a)–(c) represent the projection of the solution data points onto the (a) Y-X plane, (b) Z-X plane and (c) Z-Y plane. (d) Represent a comparison of time-history plots of $Y(t)$ by present method and RK4
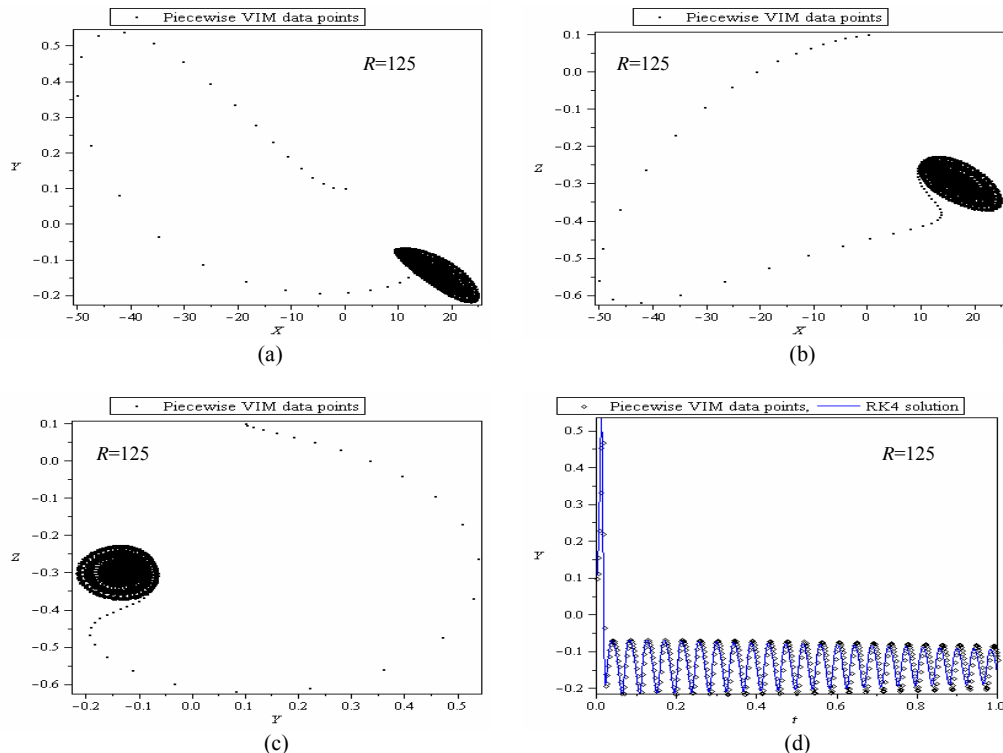
Fig. 4. The evolution of trajectories over time in the state space for *R*=30 of steady fixed point≈ (−7.77, 0.26, −0.25).
The graphs (a)–(c) represent the projection of the solution data points onto the (a) *Y-X* plane, (b) *Z-X* plane and (c) *Z-Y* plane. (d) Represent a comparison of time-history plots of *Y*(*t*) by present method and RK4

Fig. 5. The evolution of trajectories over time in the state space for *R*=125 of steady fixed point≈ (17.39, −0.14, −0.3).
The graphs (a)–(c) represent the projection of the solution data points onto the (a) *Y-X* plane, (b) *Z-X* plane and (c) *Z-Y* plane. (d) Represent a comparison of time-history plots of *Y*(*t*) by present method and RK4
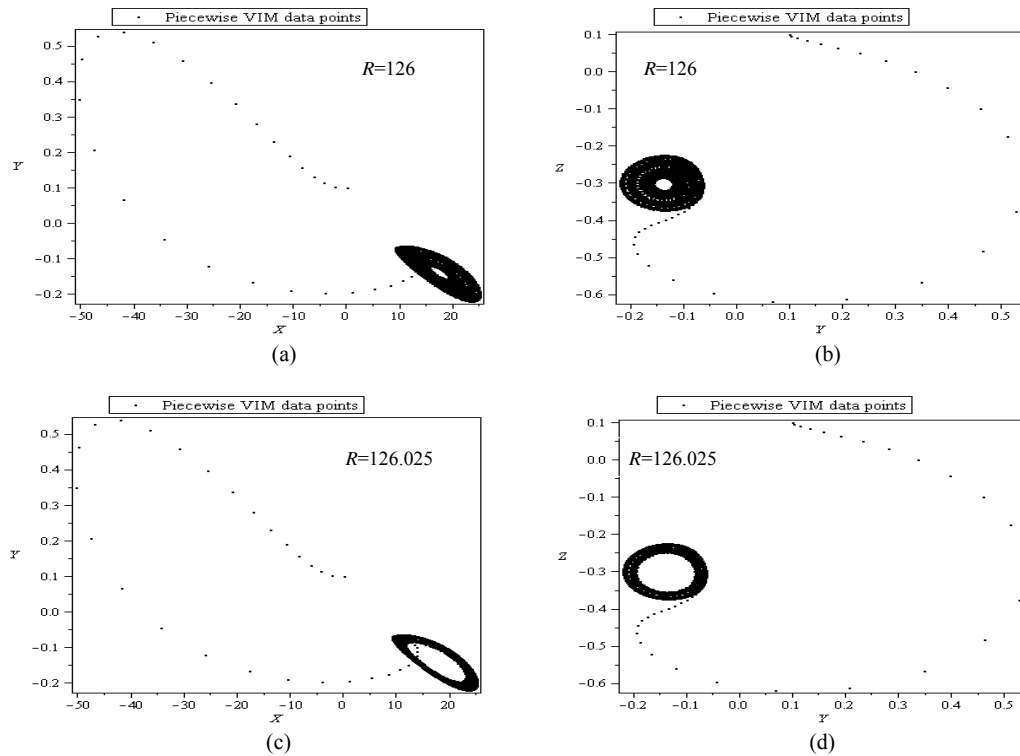
Fig. 6. The evolution of trajectories over time in the state space. The graphs (a) and (b) represent the projection of the solution data points onto the (a) *Y-X* plane and (b) *Z-Y* plane for *R*=126. The graphs (c) and (d) represent the projection of the solution data points onto the (c) *Y-X* plane and (d) *Z-Y* plane for *R*=126.025
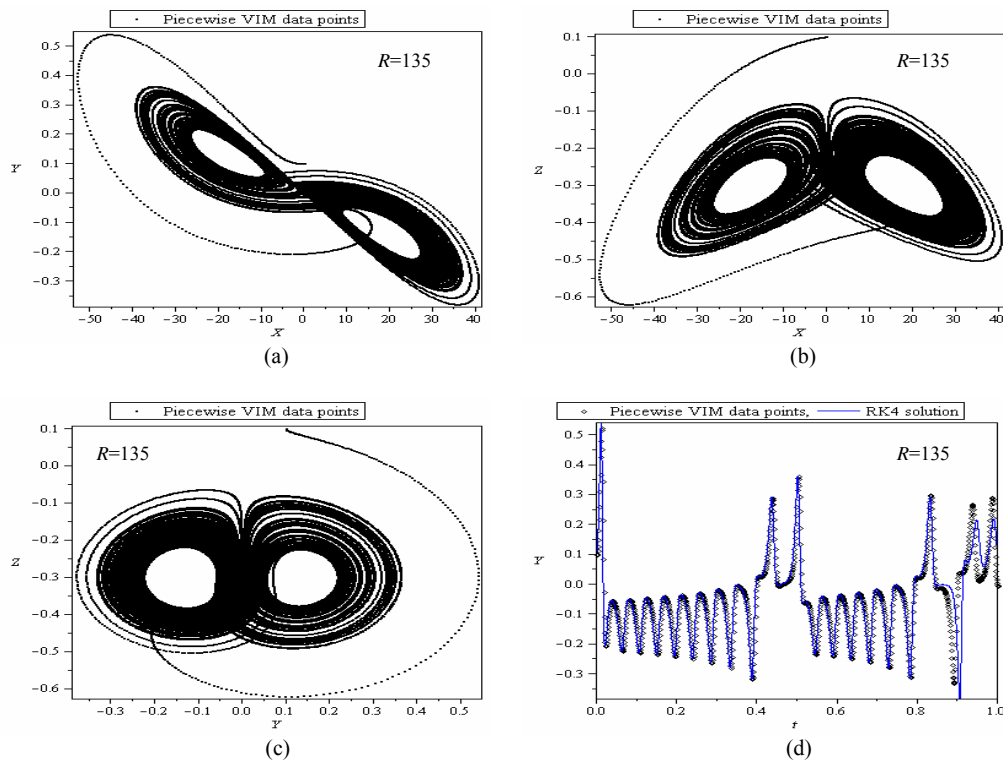

Fig. 7. The evolution of trajectories over time in the state space for *R*=135. The graphs (a)–(c) represent the projection of the solution data points onto the (a) *Y-X* plane, (b) *Z-X* plane and (c) *Z-Y* plane. (d) Represent a comparison of time-history plots of *Y*(*t*) by VIM and RK4
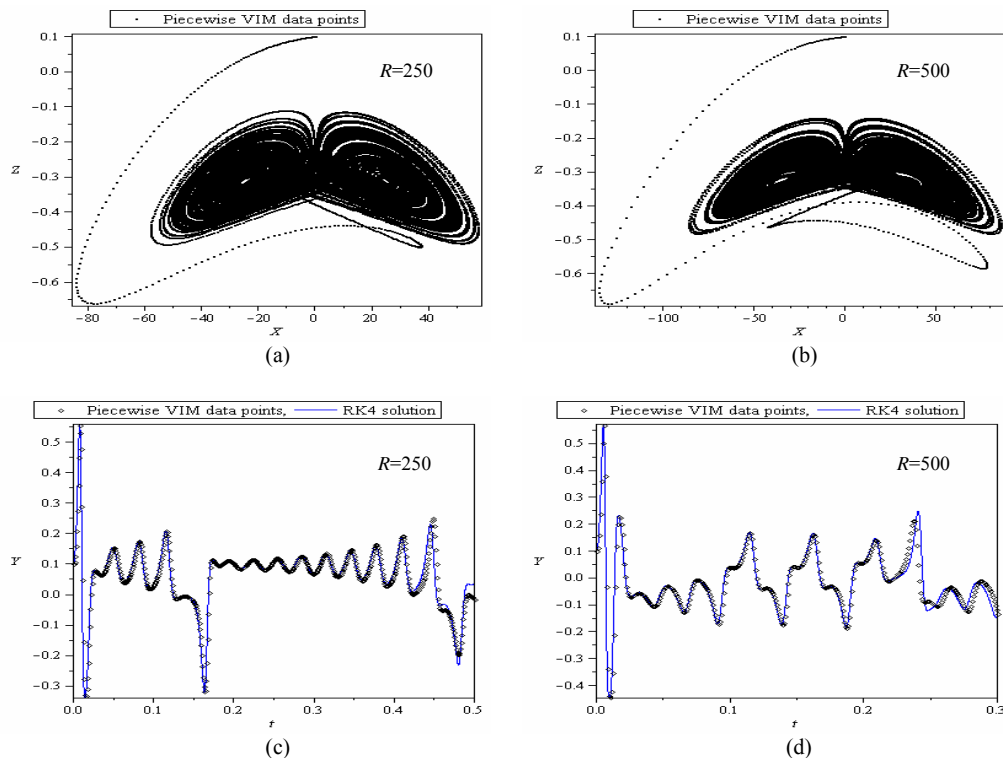
Fig. 8. The evolution of trajectories over time in the state space representing the projection of the solution data points onto the *Z-X* plane for *R*=250 in (a) and *R*=500 in (b); and a comparison of time-history plots of *Y(t)* by piecewise VIM and RK4 for *R*=250 in (c) and *R*=500 in (d)

VI. CONCLUSION

In this work, the piecewise VIM was proposed for investigating the transition from steady convection to chaos in a fluid saturated porous layer heated from below and solving any other highly chaotic systems such as the well-known Lorenz system. The critical value of Rayleigh number at which the model system goes to instability and chaos occurs is obtained analytically and computationally. The results show that the transition from steady convection to chaos is sudden. Comparisons between the solutions of the proposed method and the fourth-order Runge–Kutta numerical solutions were made. Form both nonchaotic and chaotic cases studied, it is evident that only two iterations approximate solutions of the piecewise VIM achieve comparable accuracy compared with the RK4 solutions for the same time step. The piecewise VIM solutions were computed via a simple algorithm without any need for special transformations, linearization or discretization. Finally, the authors are presently working towards the development of a piecewise VIM-like finite element (spatial) discretization scheme for nonlinear partial differential equations.

REFERENCES

[1] D. A. Nield and A. Bejan, *Convection in porous media*, Springer, New York, 2006.
[2] M. D. Graham and P. H. Steen, Plume formation and resonant bifurcations in porous-media convection, *J. Fluid. Mech.,* vol. 272, pp. 67–89, 1994.
[3] A. S. M. Cherkaoui and W. S. D. Wilcock, Characteristics of high Rayleigh number two-dimensional convection in an open-top porous layer heated from below, *J. Fluid. Mech.,* vol. 394 pp. 241–260, 1999.
[4] L. Kadanoff, Turbulent heat flow: Structures and scaling, *Physics Today,* vol.54, pp. 34–39, 2001.
[5] J. Otero et al., High-Rayleigh-number convection in a fluid-saturated porous layer, *J. Fluid Mech.,* vol. 500, pp. 263–281, 2004.
[6] E. N. Lorenz, Deterministic non-periodic flows, *J. Atmos.Sci.,* vol. 20, pp. 130–141,1963.
[7] P. Vadasz and S. Olek, Weak turbulence and chaos for low Prandtl number gravity driven convection in porous media, *Transport in Porous Media,* vol. 37, pp. 69–91,1999.
[8] J.-H. He, Approximate analytical solution for seepage flow with fractional derivatives in porous media, *Comput. Meth. Appl. Mech. Eng.,* vol. 167, pp. 57–68, 1998.
[9] J.-H. He, Approximate solution of nonlinear differential equations with convolution product nonlinearities, *Comput. Meth. Appl. Mech. Eng.,* vol. 167, pp. 69–73, 1998.
[10] J.-H. He, Variational iteration method—a kind of non-linear analytical technique: some examples, *Int. J. Non-linear Mech.,* vol. 34, pp. 699–708, 1999.
[11] V. Marinca, An approximate solution for one-dimensional weakly nonlinear oscillations, *Int. J. Non-linear Sci. Numer. Simul.,* vol. 3, pp. 107–110, 2002.
[12] M. A. Abdou and A. A. Soliman, Variational iteration method for solving Burger's and coupled Burger's equations, *J. Comput. Appl. Math.,* vol. 181(2), pp. 245–51, 2005.

[13] S. Abbasbandy, An approximation solution of a nonlinear equation with Riemann-Liouville's fractional derivatives by He's variational iteration method, *J. Comput. Appl. Math.,* vol. 207(1), pp. 53–58, 2007.

[14] S. Abbasbandy, A new application of He's variational iteration method for quadratic Riccati differential equation by using Adomian's polynomials, *J. Comput. Appl. Math.,* vol. 207(1), pp. 59–63, 2007.

[15] S. Momani and S. Abuasad, Application of He's variational iteration method to Helmholtz equation, *Chaos, Solitons & Fractals,* vol. 27(5), pp. 1119–1123, 2006.

[16] Z. M. Odibat and S. Momani, Application of variational iteration method to nonlinear differential equations of fractional order, *Int. J. Non-linear Sci. Numer. Simul.,* vol. 7(1), pp. 27–34, 2006.

[17] A.-M. Wazwaz, The variational iteration method for rational solutions for KdV, *K*(2,2), Burgers, and cubic Boussinesq equations, *J. Comput. Appl. Math.,* vol. 207(1), pp. 18–23, 2007.

[18] M. Tatari and M. Dehghan, He's variational iteration method for computing a control parameter in a semi-linear inverse parabolic equation, *Chaos, Solitons & Fractals,* vol. 33(2), pp. 671–677, 2007.

[19] A.-M. Wazwaz, The variational iteration method for exact solutions of Laplace equation, *Phys. Lett. A,* vol. 363(4), pp. 260–262, 2007.

[20] E. Yusufoglu and A. Bekir, Numerical simulation of equal-width wave equation, *Comput. Math. Appl.,* vol. 54(7-8), pp. 1147–1153, 2007.

[21] N. H. Sweilam, Fourth order integro-differential equations using variational iteration method, *Comput. Math. Appl.,* vol. 54(7-8), pp. 1086–1091, 2007.

[22] J.-H. He, Variational iteration method-some recent results and new interpretations, *J. Comput. Appl. Math.,* vol. 207(1), pp. 3–17, 2007.

[23] J.-H. He and X.-H. Wu, Variational iteration method: new development and applications, *Comput. Math. Appl.,* vol. 54(7-8), pp. 881–894, 2007.

[24] A.-M. Wazwaz, A reliable algorithm for obtaining positive solutions for nonlinear boundary value problems, *Comput. Math. Appl.*, vol. 4, pp. 1237–1244, 2001.

[25] S. Strogatz, *Nonlinear dynamics and chaos: with applications to physics, biology, chemistry, and engineering*, Addison-Wesley publishing company,1994.